

# A Metal-Free and Biotically Degradable Battery for Portable Single-Use Applications

Juan Pablo Esquivel,\* Perla Alday, Omar A. Ibrahim, Belén Fernández, Erik Kjeang, and Neus Sabaté

This article presents a new approach for environmentally benign, low-cost batteries intended for single-use applications. The proposed battery is designed and fabricated using exclusively organic materials such as cellulose, carbon, and wax and features an integrated quinone-based redox chemistry to generate electricity within a compact form factor. This primary capillary flow battery is activated by the addition of a liquid sample and has shown continuous operation up to 100 min with an output voltage that can be conveniently scaled to match the voltage needs of portable electronic devices (1.5–3.0 V). Once depleted, the battery can be disposed of without the need for any recycling facility, as its components are nontoxic and shown to be biotically degradable in a standardized test. The practical utility of the battery is demonstrated by direct substitution of a lithium ion coin cell in a diagnostic application.

## 1. Introduction

The use of electronic devices has experienced a tremendous rise in the past three decades and consequently, so has the rate of

Dr. J. P. Esquivel, P. Alday, Prof. N. Sabaté  
Instituto de Microelectrónica de Barcelona  
IMB-CNM (CSIC)  
C/ del Til·lers. Campus Universitat Autònoma de Barcelona (UAB)  
08193 Bellaterra, Barcelona, Spain  
E-mail: juanpablo.esquivel@csic.es


Dr. J. P. Esquivel  
Department of Bioengineering  
University of Washington  
Seattle, WA 98195, USA

O. A. Ibrahim, Prof. E. Kjeang  
Fuel Cell Research Lab (FCReL)  
School of Mechatronic Systems Engineering  
Simon Fraser University  
Surrey BC V3T 0A3, Canada

Dr. B. Fernández  
GIRO Joint Research Unit IRTA-UPC  
Torre Marimon  
08140 Caldes de Montbui, Barcelona, Spain

Prof. N. Sabaté  
Catalan Institution for Research and Advanced Studies (ICREA)  
Passeig Lluís Companys 23, 08010 Barcelona, Spain

This is an open access article under the terms of the Creative Commons Attribution-NonCommercial License, which permits use, distribution and reproduction in any medium, provided the original work is properly cited and is not used for commercial purposes.

 The ORCID identification number(s) for the author(s) of this article can be found under <http://dx.doi.org/10.1002/aenm.201700275>.

DOI: 10.1002/aenm.201700275

waste electrical and electronic equipment (WEEE) generated after their disposal. The large quantities of WEEE and the wide variety of materials they often contain (ferrous metals, nonferrous metals, noble-metal, chemicals, glass, and plastics) have raised a serious alarm on their potential adverse health and environmental consequences when incorrectly disposed of. Moreover, this waste can be regarded as a resource of valuable materials (e.g., Au, Pt, Li) that if not recovered, has to be extracted again, resulting in natural resource depletion and environmental degradation. Recovering these metals and satisfying the demand for cheap second-hand equipment has become profitable

business in emerging economies, which has turned Asia (in particular, China and India) and Africa into recipients of 90% of globally exported WEEE.<sup>[1]</sup> However, dismantling procedures are often carried out in inappropriate infrastructures with discarded components being openly incinerated and disposed of in unlined landfills that lack monitoring of leachate recovery systems of any kind. Due to their content of heavy metals, batteries are one of the most hazardous components of e-waste. For this reason, many Organization of Economic Cooperation and Development (OECD) countries have established regulations on the maximum permitted content of certain metals such as mercury or cadmium and the mandatory recycling of spent batteries.<sup>[2]</sup>

Lithium-ion batteries are today the most predominant energy sources in portable applications because of their high energy density, low sensitivity to temperature variations, and no memory effect when recharging.<sup>[3]</sup> However, they are starting to raise important concerns related to the relatively low abundance of lithium metal—which is likely to increase the environmental impact of its extraction methods—and the large amount of CO<sub>2</sub> generated during battery manufacturing. In fact, its life cycle assessment determines that the use of lithium is only justified in rechargeable applications beyond hundreds of cycles, which clearly prohibits its use as primary batteries.<sup>[3,4]</sup> Despite all these worrying facts, battery recycling is far from meeting the goals set in developed regions (less than 30% of sold batteries are collected for proper recycling) and it is practically inexistent in low resource settings.<sup>[5]</sup> The most alarming issue is that consumption of batteries is expected to rise significantly in the following years due to the growth of small-sized portable appliances in the Information and Communications Technology

(ICT) sector. Generally, these devices are powered by primary cells that are to be disposed of after depletion. This means a future rise in the number of batteries that will be discarded in an uncontrolled way—and almost fully charged in case of applications with short duration such as single use point-of-care devices. In view of this perspective, tightened environmental laws and increased provisions for recycling infrastructure (primary battery collection and processing) are urgently needed. However, this approach is not conducive in the short-term in developing economies due to the high cost and complexity of implementation. Indeed, this may not be environmentally sustainable even for developed economies; building up costly and energy-consuming recycling plants to take care of the batteries generated along the linear “take–make–dispose” path followed traditionally since the early days of industrialization entails a huge waste of natural resources, energy, and labor. In this sense, the approach of the circular economy—which aims to minimize, track, and eliminate the use of toxic chemicals and waste through careful device design and conception—appears to be a promising way to meet the technological needs of current society without compromising future generations.

In this regard, green electronics is an emerging area of research aimed at creating new methods and processes for the production of environmentally friendly electronics. This area is completely aligned with the circular economy principles as it specifically targets components that do not cause exhaustion of natural elements, do not require large amounts of energy to be produced, do not produce toxic by-products during their manufacture, and feature biodegradability in mild degradation conditions at the end of their life cycle. Such components would thus bypass the need for complex recycling structures and associated investments.<sup>[6]</sup>

Despite their key role in electronic devices, very few battery prototypes able to meet the requirements of green electronics have been developed to date. For *in vivo* applications, relevant innovative concepts have been presented, e.g., Kim et al. reported an edible water activated sodium battery based on melanin<sup>[7]</sup> and Yin et al. showed the abiotic degradation of a polymer encapsulated battery that uses metals like Mg, Fe, W, and Mo as electrodes.<sup>[8]</sup> These batteries are developed for implantable or edible applications and thus designed to be innocuous to the human body when decomposed in their primary elements in a short time after having been implanted or eaten. The rationale behind these devices is to make use of different nontoxic materials (both organic and inorganic) that once dissolved in the body, do not exceed the recommended dietary allowance. Other promising transient battery approaches for *ex vivo* applications have been recently reported. For example, Ding and Yu support the use of hydroquinone as metal-free, inexpensive redox-active organic materials for environmental-friendly, cost effective sustainable energy storage. Nevertheless, the reported battery still relies on an anode reaction based on the intercalation and deintercalation process of Li ions in graphite and a NASICON type Li-ion-conducting solid membrane LATP as separation membrane.<sup>[9]</sup> Fu et al. reports another example of transient battery with high power density, which contains a lithium anode, a vanadium oxide cathode, and indium tin oxide as conducting material. Although these materials may present toxicity concerns for environment and human health, the article completely

neglects what would be the impact of the battery after its degradation in water under unregulated conditions (i.e., rivers, lakes, landfills, etc.).<sup>[10]</sup> Recent works on paper fuel cells based on biocatalysts such as microbes and enzymes have opened a new alternative to sustainable power sources. However, there are still many challenges to overcome regarding their reproducibility, signal stability, and power density to meet energy requirements of portable electronics.<sup>[11]</sup> The field of supercapacitors has also experienced relevant activity toward the use of environmentally benign fabrication processes and materials, such as cellulose and carbon.<sup>[12]</sup> A recent article by Chen et al. reports an asymmetric supercapacitor based on wood carbon anode, a wood separation membrane, and a MnO<sub>2</sub>/wood carbon cathode. The article shows noteworthy results as an energy storage device with high energy and power density where most of its components could be biodegraded.<sup>[13]</sup> These examples evidence the diverse efforts in portable energy storage research toward more environmentally respectful solutions.

The present work introduces a new concept of single-use primary battery specifically made to power small electronic devices that when disposed of, breaks down into simple compounds as a result of the biotic degradative processes of microorganisms present in soils and natural water bodies. This means that unlike the previous examples of transient batteries where only some components were dissolvable in saline solutions or degraded due to self-corrosion processes, this battery has the potential to undergo complete mineralization of its chemicals to CO<sub>2</sub>, CH<sub>4</sub>, H<sub>2</sub>O, and N<sub>2</sub>, which allows the battery to effortlessly close its cycle back to nature.

The presented battery is completely built upon organic materials made of cellulose, carbon paper, beeswax, and organic redox species and can be fabricated by affordable methods with low energy consumption. Once activated, the battery is set to operate for a certain amount of time—up to 2 h—and then be disposed of in an organic waste container or even discarded in the field, where it will biotically degrade by bacteria with a minimal environmental impact.

In order to show its outstanding capabilities, six different research challenges pertaining to battery development are addressed in this work: device design, chemistry selection, battery operation, voltage scalability, practical application, and effective biotic degradation. Proposed solutions to each of these six challenges are outlined in the following sections.

## 2. Results

### 2.1. Device Design

We hereby introduce the PowerPAD (Power: Portable And Disposable), a fully organic and completely biodegradable battery concept inspired by the sustainability principles of green electronics. As illustrated schematically in **Figure 1**, the PowerPAD concept<sup>[14]</sup> represents a new class of batteries designed to operate for relatively short periods of time (from minutes to 1–2 h) to fulfill the power needs of portable applications while not requiring any specific recycling facility for its disposal. The PowerPAD design, as well as its acronym, is inspired from a traditional notepad made from a stack of paper sheets, i.e.,

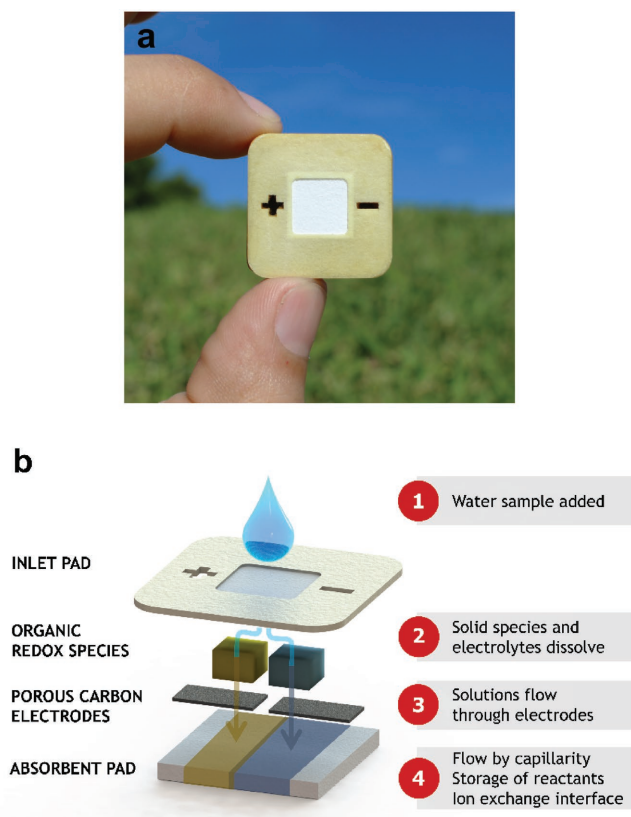


**Figure 1.** PowerPAD biodegradable battery: a) actual photograph and b) conceptual schematic of relevant components and working principle.

layered organic materials. The battery is thus designed using organic materials such as cellulose, carbon paper, and beeswax that can be fabricated by affordable methods with low energy consumption and layered to form an integrated device. Energy is stored in the form of water-soluble organic redox species inside the pad, representing two dormant electrochemical half-cells. The battery is activated by the addition of a liquid sample that dissolves the reactants and carries them to the electrodes by capillary flow. After electrochemical discharge of power, the device can be disposed of together with organic waste or even discarded on the ground for natural decomposition, as it comprises exclusively biodegradable materials and does not contain any metals, plastics, or harmful substances. In summary, the proposed battery function comprises three simple steps: (1) add water; (2) extract power; and (3) dispose of.

More specifically, the proposed biodegradable battery is designed as a vertical capillary flow cell. As shown in Figure 1, the device structure is composed of several patterned cellulose layers that when stacked together define the microfluidic paths of the cell and the compartments that house the electrodes and reactant compounds. In order to render the structural parts rigid and impermeable, the cellulose is impregnated with natural beeswax, which allows creating hydrophobic areas in a selective manner. The top structural cellulose layer hosts a central inlet pad able to receive an external liquid sample.

Underneath this pad, two separated small reservoirs contain the positive and negative redox species and the supporting

electrolytes originally stored in the solid state. The two electrodes made of hydrophilic porous carbon paper are placed below the respective reactant reservoirs and sandwiched between two thin layers of cellulose in order to ensure reliable capillary flow of reactants through the electrodes and into the large cellulose absorbent pad at the bottom. The outward facing surfaces of the device are sealed with a beeswax-covered cellulose layer in order to prevent liquid leakages. The electrodes are accessed via the positive and negative terminals on the top surface of the device in order to connect a load. The proposed battery is conceived as a single use power source that is activated by the addition of a small sample of liquid, such as water, urine, or saliva, on the inlet cellulose pad. When the inlet pad is saturated, water flows by capillarity to each of the reservoirs and dissolves the stored redox species and electrolytes. Once dissolved, the reactant species flow through the porous carbon electrodes toward the absorbent pad. The battery starts generating power when the two electrolytes get in contact at the absorbent pad. This pad has an important role in the device function as it establishes the capillary flow that makes the species flow through the electrodes while also providing electrolytic contact between the two electrochemical half-cells. Due to the colaminar flow established by capillarity in the paper sheets, the two reactant streams are effectively separated after activation of the battery and start mixing only by diffusion at their contact interface.<sup>[15]</sup> Taking into account the diffusion coefficient of the redox species in aqueous media ( $\approx 10^{-6} \text{ cm}^2 \text{ s}^{-1}$ ) and the distance between the electrodes (2 mm), no significant crossover of reactants is expected during the battery operation time, which ranges from minutes to a few hours. Furthermore, this time could even be extended by engineering capillary microfluidics to sustain a flow of reactants for longer times. Consequently, the proposed battery can operate effectively without an ion-conducting membrane otherwise used to separate the electrodes, which is particularly critical in the present case considering that most membranes are made from specialized polymer films that are not readily biodegradable. Furthermore, the capillary flow enables convenient integration of flow-through porous electrodes, which have been shown to deliver drastic performance improvements compared to flow-over and planar electrodes by means of high active surface area and internal mass transport rates.<sup>[16]</sup> The provision of flow in the form of a redox capillary flow battery thus contributes three critical services that together enable the unique function of the PowerPAD: (1) activation; (2) membrane elimination; and (3) high-performing electrodes. Finally, it is noteworthy that the passive capillary flow facilitated by the device eliminates the need for an external pump otherwise required to drive the flow of electrolyte, and hence does not add any overhead or parasitic power consumption.

## 2.2. Chemistry Selection

In order to meet the PowerPAD requirements, the redox species used as reactants in the positive and negative half-cells should be biodegradable (preferably organic) and exist in solid form in the desired redox state at ambient conditions. They should also be soluble in water or other desired electrolytes in order to be dissolved and delivered to the electrodes during

device operation. Their electrochemical reactions should also be compatible with catalyst-free porous carbon electrodes and have fast kinetics.

Organic quinone redox species have recently captured the attention of the flow battery research community, owing to their eco-friendly, nature-inspired redox reactions with fast kinetics and low cost.<sup>[17]</sup> These quinone compounds match the majority of the requirements for the proposed battery. However, the quinone species available commercially are not in the desired redox state for discharge, which means that an initial charging step would be required to meet the current application requirements. In order to circumvent this issue, the strategy of mixed-media electrolyte conditions is deployed, wherein an acidic positive half-cell can be combined with an alkaline negative half-cell. This operational scheme is uniquely enabled by membrane-less devices such as colaminal flow cells,<sup>[18]</sup> in which reactant separation is “virtually” enabled by a colaminal flow interface, and the choice of media is not dictated by the membrane chemistry. In the present case, this facilitates the use of a broader range of commercially available redox chemistries for each half-cell. Furthermore, the proposed mixed-media condition with an acidic cathode and an alkaline anode offers two additional, significant benefits for the PowerPAD concept: (i) an increased Nernstian cell potential between the two electrodes,<sup>[19]</sup> which boosts the cell performance; and (ii) an opportunity for neutralization of the electrolytes after complete mixing in the downstream absorbent pad, which supports safe disposal. Hence, a fully organic, catalyst- and membrane-free safely disposable cell chemistry can be developed by tuning the supporting electrolyte compositions in a stoichiometric balance for complete neutralization after discharge.

Oxalic acid ( $C_2H_2O_4$ ) is accordingly selected as supporting electrolyte for the positive half-cell since it is a strong acid available in solid form that can be deposited and stored in the paper, and is an organic phytochemical present in plants and predicted to have ready biodegradability according to the US Environmental Protection Agency’s EPISuite.<sup>[20]</sup> The solubility of  $C_2H_2O_4$  in water is found to be 1 M, which is hence taken as the target concentration for the PowerPAD device. Similarly, potassium hydroxide (KOH) is selected as supporting electrolyte for the negative half-cell, as it is available in solid form for onboard storage and has high solubility and ready biodegradability prediction. A target KOH concentration of 2 M is used in order to match the 2 M protonic charge contributed by the diprotic oxalic acid for neutralization and safe disposal. As a screening approach, prospective quinone redox species that are stable in these media and available in the correct oxidation state are evaluated by linear sweep voltammetry in a conventional three-electrode electrochemical cell with various supporting electrolyte conditions. The express purpose of these measurements is to investigate the half-cell open circuit potential (OCP) and qualitatively assess the kinetics of the redox reactions on catalyst-free carbon electrodes and the effect of different supporting electrolytes.

The preliminary screening of redox chemistries identified a suitable pair of commercially available quinone species, comprising of *p*-benzoquinone (pBQ) at the positive side and hydroquinonesulfonic acid potassium salt ( $H_2BQS$ ) at the negative side. These species are selected for the proof-of-concept

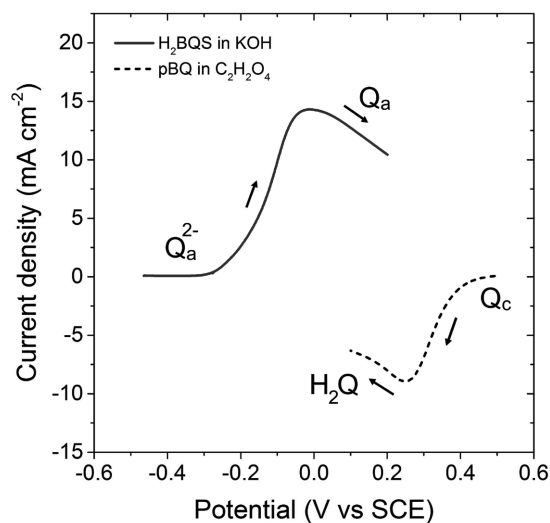


**Figure 2.** IR-compensated linear sweep voltammograms of the proposed all-organic redox chemistries representing oxidation of 0.2 M  $H_2BQS$  in 2 M KOH at the negative electrode and reduction of 0.2 M pBQ in 1 M  $C_2H_2O_4$  at the positive electrode.

as they are the most convenient off-the-shelf forms of quinones/hydroquinones with two ketone/phenol groups. The simplicity of the compounds enables good solubility, which is desired for PowerPAD operation. In addition, benzoquinones are predicted to have ready biodegradability according to EPISuite<sup>[20]</sup> and other published works.<sup>[21]</sup> The electrochemical reactions of the quinone species used for this work were previously studied and shown to have reversible redox reactions.<sup>[22]</sup> In acidic conditions, the redox reactions involve a single-step two electron two-proton process, while in alkaline conditions, the redox reactions involve two electrons process with no proton involved.<sup>[19,23]</sup> A target concentration of 0.2 M is taken, close to the solubility limit of these species. The obtained IR-compensated voltammograms for the negative (0.2 M  $H_2BQS$  in 2 M KOH) and positive (0.2 M pBQ in 1 M  $C_2H_2O_4$ ) half-cells are provided in **Figure 2**. The result shown is a representation of the intended discharge electrochemical reactions immediately following species dissolution during PowerPAD operation. These reactions correspond to the oxidation of deprotonated  $H_2BQS$  ( $BQS^{2-}$ ) in KOH at the negative half-cell and the reduction of pBQ in  $C_2H_2O_4$  at the positive half-cell. The OCPs are measured to be  $-0.46$  and  $0.49$  V versus saturated calomel electrode (SCE) for the negative and positive half-cells, respectively, suggesting a possible discharge cell potential window up to  $\approx 1$  V for the combined cell reaction. The results also indicate rapid electrochemical kinetics for both half-cells on the pure carbon electrodes. The slightly lower peak observed for pBQ can be explained by the somewhat lower solubility found for pBQ compared to  $H_2BQS$ . Based on these findings, the proposed cell chemistry is deemed adequate for the PowerPAD application.

### 2.3. Battery Operation

As per the previously described PowerPAD design (Figure 1), the proposed biodegradable battery activates upon the addition



of a liquid that dissolves the reactants stored within the device in solid form. The dissolved reactants are carried by capillary flow through the electrodes, where the electrochemical reactions take place, and into an absorbent pad at the bottom of the device. The battery operation is thus a transient process that starts upon reactant dissolution and continues for a period of time until the reactants are consumed or mixed internally, thereby causing the output voltage to drop below a certain cut-off value. Provided the passive nature of the device operation once liquid is added, the flow characteristics are fundamentally controlled by the geometrical features and surface properties of the internal materials, while the reactant concentrations are controlled by the relative dissolution rates. In order to decouple these effects, the device is first characterized with reactants in premixed solutions at the defined target concentrations based on their solubility. This approach is used to demonstrate the overall flow battery operation and to evaluate the impact of the absorbent pad dimensions on the battery performance. This pad plays an important role, as it drives the capillary flow, defines the ion-exchange interface, and serves as storage of dissolved reactants. Four different absorbent pads with varying thickness ( $h$ ) are tested (Figure S1, Supporting Information).

The total volumes of solutions added to the batteries for each measurement are 170, 390, 740, and 1440  $\mu\text{L}$  for absorbent pad thicknesses of  $h/2$ ,  $h$ ,  $2h$ , and  $4h$ , respectively, in order to reach saturation of the internal components. The open circuit voltage (OCV) of the batteries is continuously measured after adding the solutions, reaching a pseudo-steady state value of  $0.75 \pm 0.05$  V in all cases. Polarization curves for battery discharge are measured once the solutions are completely absorbed in the absorbent pad, with results shown in Figure 3. It is observed that the maximum power delivered by the battery increases with the absorbent pad thickness, reaching a maximum value of  $1.7 \pm 0.2$  mW with the thickest pad ( $4h$ ).

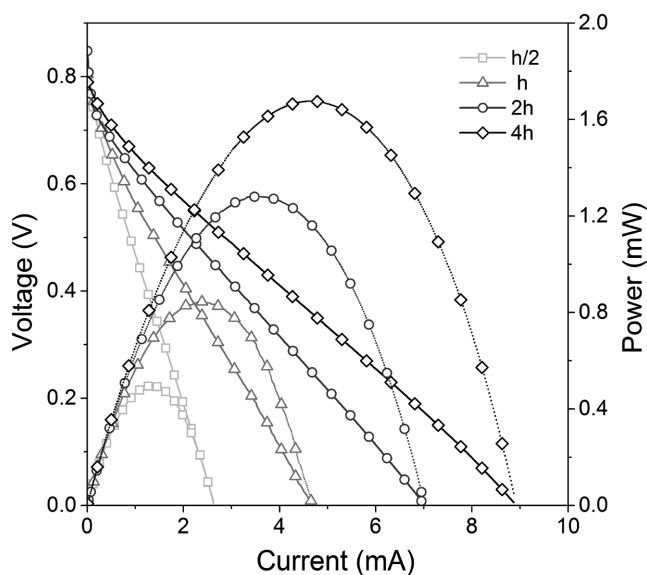


**Figure 3.** Discharge polarization curves of biodegradable redox capillary flow battery prototypes with four different absorbent pad thicknesses (as indicated;  $n \geq 3$ ) supplied with premixed solutions of 0.2 M  $\text{H}_2\text{BQS}$  in 2 M KOH and 0.2 M pBQ in 1 M  $\text{C}_2\text{H}_2\text{O}_4$  at the negative and positive electrodes, respectively, at room temperature.

Based on the geometrical electrode area of  $0.25 \text{ cm}^2$ , the battery yields a maximum power density of  $6.8 \pm 0.5 \text{ mW cm}^{-2}$  at a current density of  $18.9 \text{ mA cm}^{-2}$ , which is comparable to the power densities of large-scale redox flow batteries with all-quinone chemistry<sup>[17a]</sup> and at least an order of magnitude higher than any biodegradable battery reported so far.<sup>[7,8]</sup> The significant rise in power output obtained by increasing the absorbent pad thickness is primarily attributed to the reduced internal cell resistance associated with the increased cross-sectional area for ion conduction in the pad. This can be qualitatively observed by the changes in the linear slope of the polarization curves as the pad thickness is increased.

Next, continuous battery operation is characterized by measuring discharge curves for different external loads (0.5, 1, and 2 k $\Omega$ ). The battery cut-off voltage is set to 0.5 V, representing two-thirds of the original OCV. Figure 4 shows the discharging curves obtained with the four different absorbent pad thicknesses. As expected, batteries operated at the lowest load (500  $\Omega$ ) delivered higher power values (0.50–0.85 mW) but for shorter service times (2–13 min), while batteries working under the highest load (2 k $\Omega$ ) delivered lower power outputs (0.12–0.25 mW) for longer operation times (15–85 min). For any given load, the batteries with thicker absorbent pad show better performance not only in terms of delivered power but also in operation times. The latter result is attributed to the larger amount of electroactive species stored in the pad, which enlarges the capacity of the device. The output capacity achieved with the batteries with absorbent pad thickness of  $4h$  operated under 2 k $\Omega$  load reached 0.42 mAh (Figure 4), which considerably exceeds the measured capacities of the other battery designs.

The complete, integrated battery device is then tested with redox species and electrolytes stored internally in solid form and dissolved dynamically during operation upon the addition of water on the inlet pad. For comparative purposes, the amounts of liquid (volume) and stored reactants (moles) used in these experiments are identical to those used previously in the premixed solutions for each of the four different absorbent pad thicknesses. Given that the operational nature of the device is inherently transient, its performance is evaluated solely during continuous operation in the form of complete discharge runs until the cut-off voltage is reached. The obtained discharging curves under a fixed external load of 2 k $\Omega$  are provided in Figure 5.

Overall, the results indicate that the batteries with internally stored reactants have a similar response to those operated with premixed solutions. In most cases, the batteries with internal storage initially deliver lower voltages but sustain the power output for longer times (up to 100 min). This is reasonable considering the dynamic dissolution of reactants, which is not instantaneous and rather leads to a gradual ramp in concentration of reactants flowing through the porous electrodes as a function of time. The close proximity of storage and reaction sites allowed a gradual release that counteracted the diffusive mass transport limitations during battery discharge and improved the performance at high run-times.

The high-capacity pad configuration combined with internal reactant storage provides a particularly effective solution with performance and capacity that exceed those of the premixed

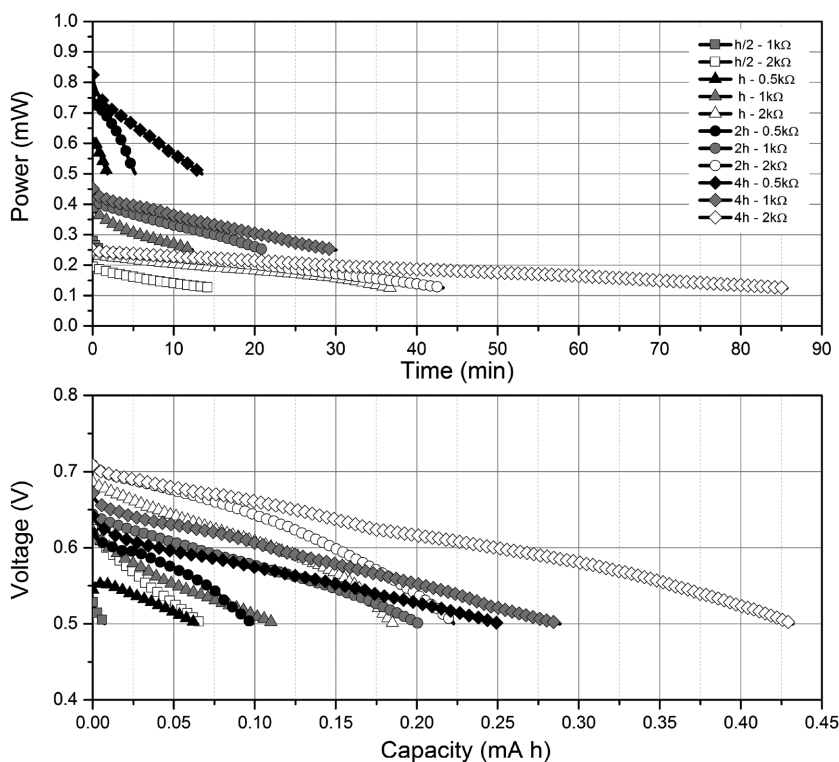


**Figure 4.** Continuously measured discharge curves of the biodegradable primary battery prototypes with four different absorbent pad thicknesses subjected to fixed external loads (as indicated;  $n = 3$ ) and a cut-off voltage of 0.5 V, using premixed solutions of 0.2 M  $\text{H}_2\text{BQS}$  in 2 M KOH and 0.2 M pBQ in 1 M  $\text{C}_2\text{H}_2\text{O}_4$  at the negative and positive electrodes, respectively, at room temperature.

reactant experiment. The operational energy density of the prototype device, based on the electrical energy generated from the discharge data in Figure 5 normalized by the mass of the stored reactants, is estimated to be  $32 \text{ Wh kg}^{-1}$ . This value compares favorably to other recently reported biodegradable batteries,<sup>[7,8]</sup> albeit further improvements are needed to reach the level of conventional primary batteries such as Li-ion batteries. An important advantage of the present device configuration, in terms of energy density, is that the reactants are stored in the dry, solid state. Compared to an equivalent redox flow battery with the same reactants stored in liquid electrolytes, the operational energy density is  $\approx 7\times$  higher. This feature is particularly important for the portable applications intended for the battery.

Figure S2 (Supporting Information) shows the Coulombic electroactive material utilization calculated from the discharge curves of the battery prototypes in Figure 5 as the fraction of active species converted by the battery during discharge until the cut-off voltage (in this case 0.5 V) is reached. The batteries with an intermediate absorbent pad thickness operated under a high load show the highest active material utilization among the tested conditions. Interestingly, under these conditions, the device with internally stored reactants achieves a higher utilization (13.3%) than the corresponding device supplied with premixed reactant solutions (8.9%), which could be due to reactions already taking place in the dissolved active species before coming into the battery. This indicates yet another advantage of the proposed PowerPAD flow battery configuration with

onboard reactant storage in terms of reactant utilization, although further optimization is required to fully exploit its potential in this regard.

## 2.4. Voltage Scalability

Most commonly used electronic applications require power delivery at higher voltage ( $\approx 2.0\text{--}3.0 \text{ V}$ ) than that produced by a single-cell battery such as the PowerPAD cell reported above. One of the strategies to obtain a higher output voltage from a battery is to stack several cells in series, which is the strategy selected here in order to demonstrate scalability. For the present PowerPAD device configuration, it is necessary to reduce the width of the absorbent pad ( $w$ ) in order to increase the number of cells within the same device footprint (Figure S1, Supporting Information). In addition, by splitting the absorbent pads, the cells within the stack are isolated electrolytically, which is practical in order to minimize internal shunt currents and losses occurring in serial stacks with electrolytic connection.<sup>[24]</sup> Single cells with different absorbent pad widths are hence analyzed as a first step in order to explore the scalability of the PowerPAD concept. Figure S3 (Supporting Information) shows the internal layers of the batteries and

Figure S4 (Supporting Information) depicts the electrode configurations in more detail. For comparative purposes, the absorbent pad volume is kept constant by increasing the thickness of the pad proportionally to the reduction in width (Figure S5, Supporting Information). Figure S6 (Supporting Information) shows the average polarization curves obtained for single cell batteries with  $1h\text{-}1w$ ,  $2h\text{-}w/2$ , and  $4h\text{-}w/4$  absorbent pad dimensions of fixed volume supplied with premixed reactant solutions. All devices show good performance with similar overall characteristics. Interestingly, however, the devices with the lowest absorbent pad width achieve the highest performance ( $1.2 \pm 0.1 \text{ mW}$  peak power), which is attributed to the greater absorbent pad thickness.

Next, batteries with absorbent pad dimensions of  $2h\text{-}w/2$  are used to assemble a 2-cell stack with a nominal output voltage of 1.5 V. In addition, a 4-cell stack with absorbent pad dimensions of  $4h\text{-}w/4$  is developed to provide a nominal output voltage of 3.0 V. The multicell stacks use the same footprint as the single cell device ( $26 \text{ mm} \times 26 \text{ mm}$ ). Each stack features two or four pairs of reactant compartments placed above the corresponding electrodes. The individual cells are connected internally in series and share a single inlet pad such that they can be simultaneously activated by a single shot of water, but use separate absorbent pads for voltage scalability. The assembled battery stack prototypes are shown in Figure 6a along with measured polarization curves in Figure 6b. The 2-cell and 4-cell stacks are observed to reach  $1.5 \pm 0.2$  and  $3.0 \pm 0.2 \text{ V}$  open circuit

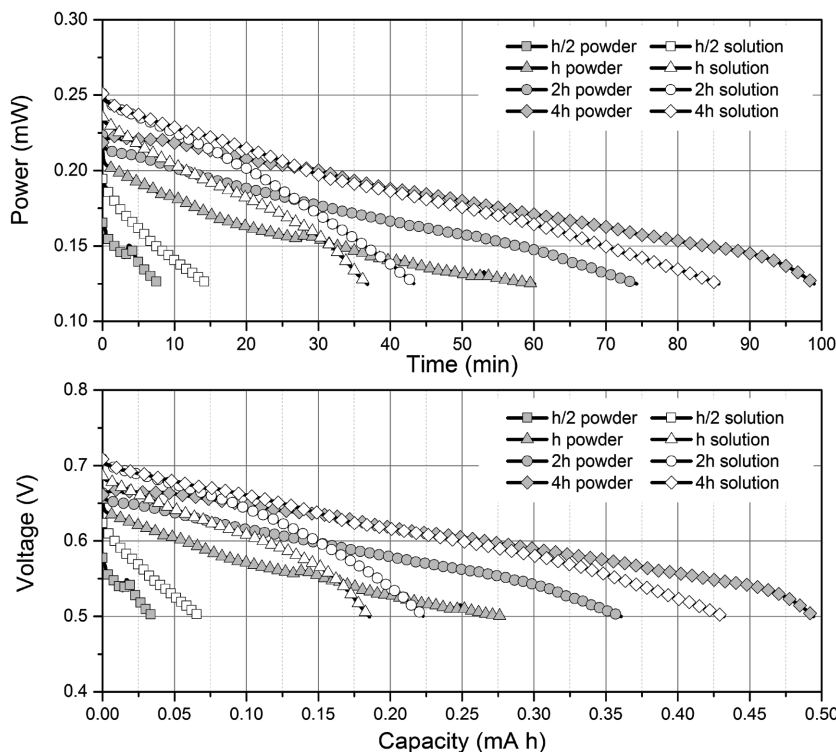


**Figure 5.** Discharge curves of integrated biodegradable primary batteries activated with water measured at room temperature for various absorbent pad thicknesses and external loads with a cut-off voltage of 0.5 V (as indicated;  $n = 3$ ). The battery prototypes contained internal storage of redox species and electrolytes in the solid state that dissolved and flowed by capillarity upon the addition of water at the inlet pad.

voltage, respectively, as intended by design. Similarly, the two stacks produce a maximum power output of  $1.5 \pm 0.1$  and  $2.8 \pm 0.1$  mW, respectively, close to the optimal doubling and quadrupling of the single cell performance.

## 2.5. Practical Application

As a proof-of-concept of the utility of the PowerPAD for practical, real-world applications, the 4-cell stack is demonstrated

as the sole power source for a portable water-monitoring instrument that usually runs with a 3 V Li-ion coin cell battery, which is now removed. The instrument measures temperature, conductivity, and total dissolved solids (TDS) in a water sample, which are typically relevant parameters in water sensing. For this experiment, two different samples are used: a sample of laboratory grade deionized water and a sample of natural water collected from a local river in Barcelona, Spain. The water analyzer is connected to the PowerPAD device and the detector is inserted into a beaker containing the water sample. A small volume of the same water sample to be analyzed is then added to the battery inlet pad for activation. An image of the water analyzer powered directly by the 4-cell PowerPAD stack, without any ancillary power conversion systems or components, is shown in Figure 7a. The current drawn by the water analyzer and the battery output voltage obtained for the two different water samples during the experiment are depicted in Figure 7b. It can be seen that the battery activated with the river sample yields a fairly similar open circuit than the one activated with deionized water. The measurement is successfully carried out after 30 s of battery activation. The analyzer requires an average current of  $\approx 0.2$  mA to continuously measure the sample and display the result on its LCD

display. Once the measurement is taken (results yielding 6 ppm TDS and  $12 \mu\text{S cm}^{-1}$  for the deionized water and 424 ppm TDS and  $958 \mu\text{S cm}^{-1}$  for the river water), the reading is stored by pushing a button of the instrument, which halts the sensing function and freezes the information in the display. During this phase, the current required by the analyzer decreases to  $\approx 20 \mu\text{A}$ . After activation, the battery voltage decreases up to 300 mV during the high current demand phase when the analyzer measures and displays the results, after which the voltage increases again to a value close to its open circuit during the

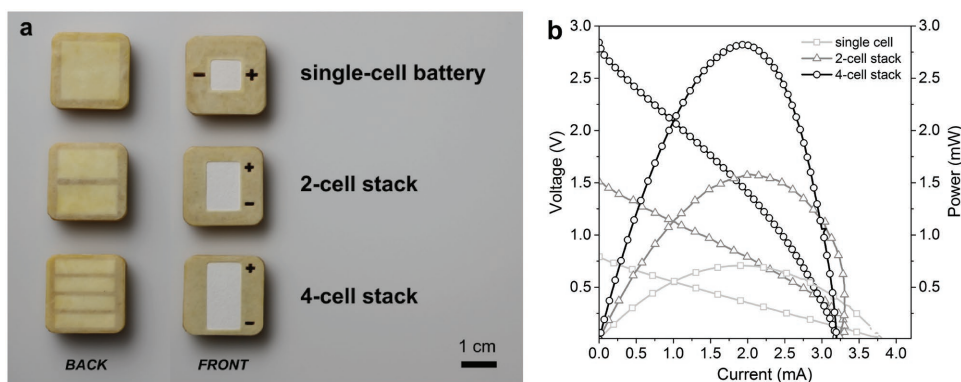


**Figure 6.** Scalability of the biodegradable redox capillary flow battery demonstrated by integration of one, two, and four cells within the same device footprint. a) Image of the assembled single cell, 2-cell stack, and 4-cell stack prototypes. b) Average polarization curves ( $n \geq 3$ ) measured with premixed reactant solutions of 0.2 M  $\text{H}_2\text{BQS}$  in 2 M KOH and 0.2 M pBQ in 1 M  $\text{C}_2\text{H}_2\text{O}_4$ .

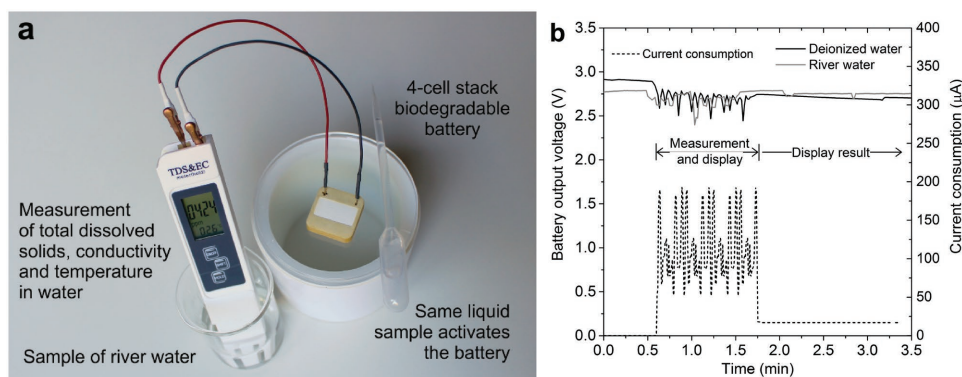


**Figure 7.** Practical utility of the biodegradable redox capillary flow battery demonstrated by powering a portable water monitoring instrument. a) Image of a portable water monitoring device powered directly by a biodegradable battery. The device analyzes a river water sample that is also used to activate the battery. b) Electric current drawn by the water monitoring device and output voltage of the battery during the measurement process.

secondary phase when the result is stored and displayed. Throughout this experiment, the PowerPAD unit is shown to reliably deliver the required levels of voltage and current for both operational phases of the measurement in the complete absence of supplementary electronics.

## 2.6. Biodegradability

The biodegradability of the PowerPAD battery, expressed as primary degradation (Dp), is determined following the guideline of the OECD Test 311<sup>[25]</sup> that comprises recommendations of other normalized tests (ISO,<sup>[26]</sup> ASTM,<sup>[27]</sup> US-EPA,<sup>[28]</sup>) and is widely used as standard test. Biodegradation is defined as a process where a material breaks down into simple compounds, such as CO<sub>2</sub>, CH<sub>4</sub>, H<sub>2</sub>O, and N<sub>2</sub>, as a result of the action of microorganisms. The assay simulates the biodegradation process under biotic anaerobic conditions of disposable devices taking into account a specific WEEE management practice. Furthermore, the low concentration of the evaluated materials in the performed test ensures that the biodegradation kinetics reflect those expected in the environment being simulated. The selection of an anaerobic test represents the worst-case scenario for the biodegradation of the batteries, as the biodegradation of cellulose-based materials is slower than that in aerobic conditions.<sup>[29]</sup> Only 5%–10% of cellulose degrades in natural environment anaerobic conditions because in the case of landfills, water-logged soils or aquatic sediments where anaerobic or anoxic environments are expected, lower rates and longer times for biodegradation are expected because the local population of microorganisms in these natural environments may be smaller than that in the biodegradability assay with an artificially induced high population.<sup>[30]</sup> The test monitors the inherent biodegradability in anaerobic conditions, expressed as the percentage of the initial total carbon mass of the material that is transformed into C-CO<sub>2</sub> and C-CH<sub>4</sub> after a minimum period of 60 d. The initial total carbon (TC) content that is biodegraded is calculated from periodic measurements of gas products and its evolution is plotted in a curve. **Figure 8** shows the evolution of the obtained biodegradation curves of the complete and blank batteries (with and without internally stored chemical

reactants), as well as the reference material (cellulose acetate). A clear plateau, indicating maximal degradation, is attained from day 40 for the batteries and from day 63 for the cellulose reference. It is noteworthy that the degradation rate of the batteries is even greater than that of pure cellulose, despite their larger particle size. All tested materials reach similar levels of biodegradation after 60 d, with values of 54% ± 4%, 46% ± 2%, and 52% ± 2% for the complete battery, blank battery, and cellulose, respectively, indicating that primary biodegradation of the studied materials occurred. These values are coherent with those reached in cellulose acetate based material biodegradation tests, with values between 40% and 60% TC under anaerobic conditions. Based on these results, the batteries can be considered biodegradable, and no toxic effects may be expected from the use of the present quinone-based redox chemistry. Therefore, according to the norm, these devices can be considered nonpersistent and assumed to degrade by microorganisms present in soils or water bodies in the medium to long term or in simple waste treatment plants or other environmental compartments in the short term.

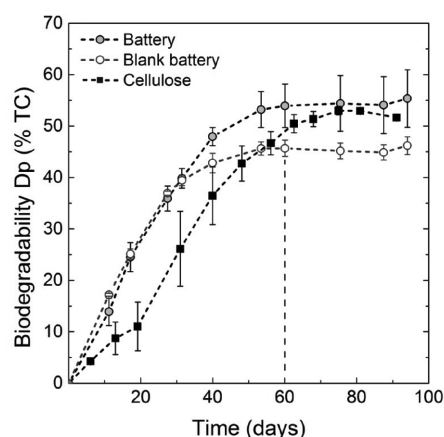


**Figure 8.** Battery biodegradability. Primary degradation (Dp) or biodegradability of complete batteries, blank batteries (without internally stored reactants), and reference material (cellulose acetate) in terms of initial total carbon content (%TC) that is biodegraded.



### 3. Discussion

The biodegradable battery prototypes presented here can operate for up to 100 min with an output voltage that can be scaled to match the voltage needs of portable electronic devices (1.5–3.0 V). Despite its working principle based on the well-known redox flow batteries, it is the first time that this principle has been explored to develop a single-use portable format with clear environmental advantages. Moreover, the technology allows further increases of both operation time and output power. It is noteworthy that even at the present laboratory stage, the prototypes have proven to readily substitute a coin cell battery in a real application, with cost of materials in the range of tens of euro/dollar cents (see Bill of Materials in Table S1 in the Supporting Information).

This new class of biodegradable, portable redox capillary flow batteries is ideally suited to provide power for a new generation of green electronic devices, and could further be explored in terms of operative design, structural materials, and chemistry. For instance, the battery half-life can be extended by engineering the absorbent pad to sustain a capillary flow of species for a longer duration. Moreover, the present battery is designed to work once and its operation is intrinsically transient. Several relevant parameters affecting its performance are time-dependent and start changing after the liquid is added; for example, the rate of dissolution of species/electrolytes, the concentration of species/electrolytes, and the flow rate of reactants. These aspects offer a rich set of parameters to further optimize in future studies.

For this proof-of-concept, beeswax was used as structural material because it is abundant, organic, inexpensive, moldable, impermeable, and mechanically robust. Furthermore, its properties can be customized for hardness and melting temperature. However, other materials such as biopolymers—olylactic acid (PLA) or polyhydroxyalkanoate (PHA)<sup>[31]</sup>—are potential alternatives to substitute beeswax. These materials, already used in the industry as biodegradable paper coatings, would confer the device a compostable characteristic and an industrially scalable fabrication process.

The redox chemistry proved for this first development was based on suitable quinone species available off-the-shelf with good kinetics on carbon. However, the device is not restricted to these species, and other commercially available candidates could be considered. Caffeic acid, a hydroquinone and antioxidant found in coffee, and water-soluble vitamin K<sub>3</sub>, a naphthoquinone, are examples of other commercially available quinone species that are available in the desired redox state for discharge. Moreover, other research groups are working on modeling the effect of functional groups on quinones.<sup>[32]</sup> For example, hydroxyl functional groups were shown to enhance solubility and reduce standard potential, which would benefit the battery anode, while sulfonic acid functional groups were shown to enhance solubility and increase standard potential, which would be beneficial for the cathode. By in-house synthesis of quinone species with custom functional groups, the number of candidates meeting the requirements of this approach could be increased and the performance of the device may be further enhanced. This would enable tailored solubility, rate of dissolution, and standard potential difference as well as

reduce the cost of chemical compounds. Furthermore, besides using quinone species, inorganic redox couples can also be suitable for this approach, while maintaining a similar or even higher cell voltage. Some of these inorganic salts may form hydroxide precipitates in alkaline media, yet are compatible for the cathode by utilizing mixed-media operation. For example, nitrates, sulfates, or phosphates are known to benefit the soils, which if combined with cheap and abundant metal redox ions, may lead to a battery that could even be compostable, adding value to the soil or water in which it is disposed of.

The biodegradability study of the PowerPAD batteries was carried out at biotic anaerobic conditions which proved their primary biodegradation. Upcoming work will include long-term biodegradability tests at aerobic conditions that could even meet the certification of home compostability.<sup>[33]</sup> Additional biodegradation tests without previous conditioning steps would be of interest such as simulation tests of regulated disposal in landfill conditions as well as unregulated disposal in soils or aquatic systems.

### 4. Conclusion

This work introduced the PowerPAD concept, a fully biodegradable battery for portable and disposable single-use applications that follows the sustainability guidelines of the circular economy. The battery was prepared using exclusively organic materials and low-energy consuming fabrication techniques. According to the results obtained in the biodegradability test, it can be disposed of in soils and waters and thus eliminate the need for recycling and the associated cost and energy consumption. Ultimately, this disposable power source concept holds great promise to radically change the portable battery paradigm; from considering it a harmful waste to a source of materials that nurture the environment, enrich soil, or remove toxins from water, far beyond the traditional life cycle of a battery.

### 5. Experimental Section

**Materials:** The chemical compounds used in this work consisted of H<sub>2</sub>BQS (H18402), pBQ (B10358), oxalic acid dihydrate (C<sub>2</sub>H<sub>2</sub>O<sub>4</sub>, O0376), KOH (P1767) (all from Sigma-Aldrich, St Louis, Missouri, USA). For the experiments using predissolved reagents, redox electrolytes were prepared at concentrations of 0.2 M H<sub>2</sub>BQS in 2.0 M KOH and 0.2 M pBQ in 1.0 M C<sub>2</sub>H<sub>2</sub>O<sub>4</sub>. During the storage of redox species in solid form within the device, an amount equivalent to the maximum solubility concentrations of the redox species was added to the compartments: H<sub>2</sub>BQS (0.023 g), pBQ (0.011 g), KOH (0.056 g), and C<sub>2</sub>H<sub>2</sub>O<sub>4</sub> (0.063 g). Each species was dissolved in 500 μL of water.

**Electrochemical Measurements:** The linear sweep voltammetry measurements were performed in a conventional three-electrode electrochemical cell. Glassy carbon electrode (0.07 cm<sup>2</sup>), platinum wire electrode, and SCE (CH instruments Inc., TX, USA) were used as working electrode, counter electrode, and reference electrode, respectively. All polarization measurements were recorded with a potentiostat (Gamry Reference 3000) at a scan rate of 5 mV s<sup>-1</sup>. The OCP of each half-cell was measured before polarization. The potential was swept from OCV in the direction of the intended discharge reaction of the measured half-cell. The solution resistance was measured at OCP using the same potentiostat and was used to perform postmeasurement IR-compensation. All chemicals were purchased from Sigma-Aldrich

(Oakville, ON, Canada) and used as received unless otherwise stated. The solutions were prepared by consecutively dissolving the supporting electrolytes and quinone species in 10 mL deionized water to the desired concentrations. The solutions were bubbled with nitrogen to minimize solution oxidation due to dissolved oxygen or ambient air.

**Device Fabrication:** The device components were designed in a CAD program (CorelDRAW, Corel, Ottawa, ON, Canada). Cellulose membranes were cut using a CO<sub>2</sub> laser cutter (Mini 24, Epilog Laser, Golden, CO, USA). Most of the device assembly was done layer by layer using alignment jigs. The structural cellulose components (238, 320, 601, CFSP223000, from Ahlstrom, Helsinki, Finland) were impregnated with melted natural beeswax (Iberceras, Madrid, Spain), which provided an impermeable coating and was also used to bond the layers. An inlet cellulose pad (238, Ahlstrom) was used to receive the liquid sample into the device. Different absorbent pad configurations were tested. A single layer of cellulose membrane 222 (Ahlstrom) with a thickness of 0.83 mm was taken as baseline material, labeled *h*. The absorbent pads *2h* and *4h* consisted of two or four layers of cellulose 222 to obtain pad thicknesses of 1.66 and 3.32 mm, respectively. In order to test a thinner pad configuration, the pad labeled as *h/2* consisted of one layer of cellulose 238 (0.34 mm thick). The electrodes consisted of porous carbon paper (TGP-120, Toray, Japan). This material has 78% porosity, with an average pore diameter around 30 μm and is 0.37 mm thick. Further details about the electrodes material and its structure and morphology may be found elsewhere.<sup>[34]</sup> The electrodes were thermally pretreated to ensure capillary flow.

**Battery Testing:** The cell voltage/current was recorded using a DropSens μStat400 bipotentiostat/galvanostat and DropView 8400 Software (DropSens S.L., Asturias, Spain). The polarization and power curves for the single cell and battery stacks were generated using linear sweep voltammetry, sweeping from the OCV to 0 V at a scan rate of 50 mV s<sup>-1</sup>. The discharging curves were recorded under different external loads of 0.5, 1.0, or 2.0 kΩ. All tests were performed at room temperature.

**Biodegradability Testing:** The assay was performed to determine the inherent biodegradability of the battery devices in anaerobic conditions. Although the main aspects were based on the OECD Test 311, the methodology also included recommendations described by Holliger et al.<sup>[35]</sup> and Angelidaki et al.<sup>[36]</sup> for anaerobic degradation tests. The test was carried out on the same type of single-cell batteries used for the electrochemical characterization, which contained H<sub>2</sub>BQS (0.023 g), pBQ (0.011 g), KOH (0.056 g), and C<sub>2</sub>H<sub>2</sub>O<sub>4</sub> (0.063 g) as stored reactants. For comparison, identical batteries without reactants were also tested, labeled as blank battery. A reference material consisting of cellulose acetate powder (CAS number 9004-35-7) was also included in the study. Prior to physicochemical characterization, four specimens of each device were shredded to a particle size of <0.5 mm in a cryogenic grinder (Freezer/Mill 6850, SPEX, Metuchen, NJ, USA). The minced devices were used for the biodegradability test in order to avoid abiotic degradation or disintegration. The materials were evaluated after being characterized by their total solids, total chemical oxygen demand, and TC content, shown in Table S2 (Supporting Information). The assay was prepared in duplicate, using glass vessels that contained 50 mL of liquid media and 70 mL of headspace. A greater headspace volume than in the OECD Test 311 was fixed in order to avoid excess overpressure inside the vessels. The initial concentration of device per vessel is given in Table S3 (Supporting Information). An anaerobic digested sludge from an urban wastewater treatment plant was used as inoculum, which was filtered to eliminate coarse materials and was kept for 7 d at 35 °C to diminish residual organic matter. The inoculum to material ratio was selected based on the OECD Test 311 recommendations (10 gTS-inoculum gTC-material<sup>-1</sup>), but a higher inoculum concentration per vessel was fixed (14.5 gTS L<sup>-1</sup>) that allowed shortening the start-up time and duration of the test. Once filled, all vessels were bubbled with nitrogen to remove oxygen and closed with gastight seals (crimp cap and septum). The assay was performed at 35 ± 2 °C for 94 d. The biodegradation was monitored through the evolution of CO<sub>2</sub> and CH<sub>4</sub> content in the gas space of the vessels as determined by gas

chromatography (Varian GC 3800, Agilent Technologies, Santa Clara, CA, USA), instead of using a pressure-measuring device and signal transducer as described in OECD Test 311. The biodegradation extent was calculated as primary degradation (D<sub>p</sub>) after 60 d and was expressed as the percentage of the initial carbon mass of the material that was transformed into C-CO<sub>2</sub> and C-CH<sub>4</sub>.

## Supporting Information

Supporting Information is available from the Wiley Online Library or from the author.

## Acknowledgements

The funding for this research provided through the Science for Solving Society's Problems Challenge by the Electrochemical Society and the Bill & Melinda Gates Foundation powerPAD is highly appreciated. J.P.E. thanks support from the Marie Curie International Outgoing Fellowship (APPOCS – GA.328144) within the 7th European Community Framework. Additional support from the Natural Sciences and Engineering Research Council of Canada (NSERC), the Canada Foundation for Innovation (CFI), and the British Columbia Knowledge Development Fund (BCKDF) is also acknowledged. E.K. acknowledges support from the Canada Research Chairs program. N.S. would like to thank financial support received from the European Research Council (BE) Grant (SUPERCCELL – GA.648518). L. Tey from the GIRO Research Unit is thanked for her support in the biodegradation tests. The authors thank Iberceras for beeswax customization.

## Conflict of Interest

The authors declare no conflict of interest.

## Keywords

biodegradable batteries, green electronics, paper microfluidics, redox flow batteries

Received: January 30, 2017

Revised: March 10, 2017

Published online: May 16, 2017

- [1] R. Widmer, H. Oswald-Krapf, D. Sinha-Khetriwal, M. Schnellmann, H. Böni, *Environ. Impact Assess. Rev.* **2005**, *25*, 436.
- [2] L. Moreno-Merino, M. E. Jiménez-Hernández, A. de la Losa, V. Huerta-Muñoz, *Sci. Total Environ.* **2015**, *526*, 187.
- [3] T. C. Wanger, *Conserv. Lett.* **2011**, *4*, 202.
- [4] D. Larcher, J. M. Tarascon, *Nat. Chem.* **2015**, *7*, 19.
- [5] F. O. Ongondo, I. D. Williams, T. J. Cherrett, *Nucl. Chem. Waste Manage.* **2011**, *31*, 714.
- [6] M. Irimia-Vladu, *Chem. Soc. Rev.* **2014**, *43*, 588.
- [7] Y. J. Kim, W. Wu, S.-E. Chun, J. F. Whitacre, C. J. Bettinger, *Proc. Natl. Acad. Sci. USA* **2013**, *110*, 20912.
- [8] L. Yin, X. Huang, H. Xu, Y. Zhang, J. Lam, J. Cheng, J. A. Rogers, *Adv. Mater.* **2014**, *26*, 3879.
- [9] Y. Ding, G. Yu, *Angew. Chem., Int. Ed.* **2016**, *55*, 4772.
- [10] K. Fu, Z. Wang, C. Yan, Z. Liu, Y. Yao, J. Dai, E. Hitz, Y. Wang, W. Luo, Y. Chen, M. Kim, L. Hu, *Adv. Energy Mater.* **2016**, *6*, 1502496.

- [11] a) F. Sharifi, S. Ghobadian, F. R. Cavalcanti, N. Hashemi, *Renewable Sustainable Energy Rev.* **2015**, *52*, 1453; b) J. Winfield, L. D. Chambers, J. Rossiter, J. Greenman, I. Ieropoulos, *J. Mater. Chem. A* **2015**, *3*, 7058; c) C. W. Narvaez Villarrubia, F. Soavi, C. Santoro, C. Arbizzani, A. Serov, S. Rojas-Carbonell, G. Gupta, P. Atanassov, *Biosens. Bioelectron.* **2016**, *86*, 459; d) M. J. González-Guerrero, F. J. del Campo, J. P. Esquivel, D. Leech, N. Sabaté, *Biosens. Bioelectron.* **2017**, *90*, 475.
- [12] L. Nyholm, G. Nyström, A. Mihranyan, M. Strømme, *Adv. Mater.* **2011**, *23*, 3751.
- [13] a) C. Chen, Y. Zhang, Y. Li, J. Dai, J. Song, Y. Yao, Y. Gong, I. Kierzewski, J. Xie, L. Hu, *Energy Environ. Sci.* **2017**, *10*, 538; b) L. Hu, J. W. Choi, Y. Yang, S. Jeong, F. La Mantia, L.-F. Cui, Y. Cui, *Proc. Natl. Acad. Sci. USA* **2009**, *106*, 21490.
- [14] J. P. Esquivel, N. Sabaté, P. Alday, E. Kjeang, O. Ibrahim, *ES Patent EP15200865* **2015**.
- [15] a) J. L. Osborn, B. Lutz, E. Fu, P. Kauffman, D. Y. Stevens, P. Yager, S. R. Narayanan, *J. Electrochem. Soc.* **2014**, *161*, A1371; b) B. Huskinson, M. P. Marshak, C. Suh, S. Er, M. R. Gerhardt, C. J. Galvin, X. Chen, A. Aspuru-Guzik, R. G. Gordon, M. J. Aziz, *Nature* **2014**, *505*, 195; c) K. Lin, Q. Chen, M. R. Gerhardt, L. Tong, S. B. Kim, L. Eisenach, A. W. Valle, D. Hardee, R. G. Gordon, M. J. Aziz, M. P. Marshak, *Science* **2015**, *349*, 1529.
- [18] a) E. Kjeang, N. Djilali, D. Sinton, *J. Power Sources* **2009**, *186*, 353; b) E. R. Choban, J. S. Spendelow, L. Gancs, A. Wiecekowsk, P. J. A. Kenis, *Electrochim. Acta* **2005**, *50*, 5390; c) R. Ferrigno, A. D. Stroock, T. D. Clark, M. Mayer, G. M. Whitesides, *J. Am. Chem. Soc.* **2002**, *124*, 12930.
- [19] M. Quan, D. Sanchez, M. F. Wasylkiw, D. K. Smith, *J. Am. Chem. Soc.* **2007**, *129*, 12847.
- [20] Environmental Protection Agency, Estimation Programs Interface Suite for Microsoft Windows, v 4.11, **2016**.
- [21] a) F. J. Enguita, A. L. Leito, *BioMed. Res. Int.* **2013**, *2013*, 14; b) K. G. Harbison, R. T. Belly, *Environ. Toxicol. Chem.* **1982**, *1*, 9.
- [22] a) M. Rafiee, D. Nematollahi, *Electroanalysis* **2007**, *19*, 1382; b) R. Gulaboski, I. Bogeski, V. Mirčeski, S. Saul, B. Pasička, H. H. Haeri, M. Stefova, J. P. Stanoeva, S. Mitrev, M. Hoth, R. Kappl, *Sci. Rep.* **2013**, *3*, 1865; c) Y. Xu, Y. Wen, J. Cheng, Y. Yanga, Z. Xie, G. Cao, presented at *2009 World Non-Grid-Connected Wind Power and Energy Conf.*, Nanjing, China, September **2009**; d) B. Yang, L. Hooper-Burkhardt, S. Krishnamoorthy, A. Murali, G. K. S. Prakash, S. R. Narayanan, *J. Electrochem. Soc.* **2016**, *163*, A1442; e) Y. Zhao, Y. Ding, Y. Li, L. Peng, H. R. Byon, J. B. Goodenough, G. Yu, *Chem. Soc. Rev.* **2015**, *44*, 7968; f) Y. Ding, Y. Li, G. Yu, *Chem. Soc. Rev.* **2011**, *2011*, 22.
- [23] P. S. Guin, S. Das, P. C. Mandal, *Int. J. Electrochem.* **2011**, *2011*, 22.
- [24] a) O. A. Ibrahim, M.-A. Goulet, E. Kjeang, *J. Electrochem. Soc.* **2015**, *162*, F639; b) B. Ho, E. Kjeang, *J. Fluids Eng.* **2013**, *135*, 021304; c) O. A. Ibrahim, M.-A. Goulet, E. Kjeang, *Electrochim. Acta* **2016**, *187*, 277.
- [25] Organization of Economic Cooperation and Development, OECD 311. *Anaerobic Biodegradability of Organic Compounds in Digested Sludge: by Measurement of Gas Production*, **2006**.
- [26] International Organization for Standardization, ISO 11734. *Water Quality: Evaluation of the ultimate anaerobic biodegradation of organic compounds in digested sludge*, **1995**.
- [27] American Society of the International Association for Testing and Materials, *E1192-92 Standard Test Method for Determining the Anaerobic Biodegradation Potential of Organic Chemicals*, **1992**.
- [28] United States Environmental Protection Agency, *Fate, Transport and Transformation Test Guidelines OPPTS 835.3400 Anaerobic Biodegradability of Organic Chemicals*, **1998**.
- [29] a) J.-D. Gu, D. Eberiel, S. P. McCarthy, R. A. Gross, *J. Environ. Polym. Degrad.* **1993**, *1*, 281; b) J. Puls, S. A. Wilson, D. Hölter, *J. Polym. Environ.* **2011**, *19*, 152.
- [30] J. Pérez, J. Muñoz-Dorado, T. de la Rubia, J. Martínez, *Int. Microbiol.* **2002**, *5*, 53.
- [31] *Metabolix*, Vol. 2016, Lowell, MA, USA **2016**.
- [32] S. Er, C. Suh, M. P. Marshak, A. Aspuru-Guzik, *Chem. Sci.* **2015**, *6*, 885.
- [33] Vinçotte, OK Compost EN 13432, **1995**.
- [34] F. C. Store, Vol. 2017, Fuel Cells Store, **2017**, Toray Carbon Paper 120.
- [35] C. Holliger, M. Alves, D. Andrade, I. Angelidaki, S. Astals, U. Baier, C. Bougrier, P. Buffière, M. Carballa, V. de Wilde, F. Ebertseder, B. Fernández, E. Ficara, I. Fotidis, J. C. Frigon, H. Fruteau de Laclos, D. S. M. Ghasimi, G. Hack, M. Hartel, J. Heerenklage, I. Sarvari Horvath, P. Jenicek, K. Koch, J. Krautwald, J. Lizasoain, J. Liu, L. Mosberger, M. Nistor, H. Oechsner, J. Vítor Oliveira, M. Paterson, A. Pauss, S. Pommier, I. Porqueddu, F. Raposo, T. Ribeiro, F. Rüsck Pfund, S. Strömberg, M. Torrijos, M. van Eekert, J. van Lier, H. Wedwitschka, I. Wierinck, *Water Sci. Technol.* **2016**, *75*, DOI: 10.2166/wst.2016.336.
- [36] I. Angelidaki, M. Alves, D. Bolzonella, L. Borzacconi, J. L. Campos, A. J. Guwy, S. Kalyuzhnyi, P. Jenicek, J. B. van Lier, *Water Sci. Technol.* **2009**, *59*, 927.